### Title

Relationships among ultrasonic and mechanical properties of cancellous bone in human calcaneus in vitro.




### Authors

Wear, Keith A
Nagaraja, Srinidhi
Dreher, Maureen L
et al.



### Publication Date

2017-10-01

### DOI

10.1016/j.bone.2017.06.021

Peer reviewed

HHS Public Access

Author manuscript

*Bone*. Author manuscript; available in PMC 2020 January 03.

Published in final edited form as:

*Bone*. 2017 October ; 103: 93–101. doi:10.1016/j.bone.2017.06.021.

# Relationships among ultrasonic and mechanical properties of cancellous bone in human calcaneus *in vitro*.

**Keith A. Wear**[a], **Srinidhi Nagaraja**[a], **Maureen L. Dreher**[a], **Saghi Sadoughi**[b], **Shan Zhu**[b], **Tony M. Keaveny**[b,c]

[a.]U.S. Food and Drug Administration, Center for Devices and Radiological Health, 10903 New Hampshire Blvd., Silver Spring, MD 20993

[b.]Orthopaedic Biomechanics Laboratory, Department of Mechanical Engineering, 5124 Etcheverry Hall, Mailstop 1740, University of California at Berkeley, Berkeley, CA 94720-1740

[c.]Department of Bioengineering, University of California, Berkeley, CA, USA

## Abstract

Clinical bone sonometers applied at the calcaneus measure broadband ultrasound attenuation and speed of sound. However, the relation of ultrasound measurements to bone strength is not well-characterized. Addressing this issue, we assessed the extent to which ultrasonic measurements convey *in vitro* mechanical properties in 25 human calcaneal cancellous bone specimens (approximately 2 × 4 × 2 cm). Normalized broadband ultrasound attenuation, speed of sound, and broadband ultrasound backscatter were measured with 500 kHz transducers. To assess mechanical properties, non-linear finite element analysis, based on micro-computed tomography images (34-micron cubic voxel), was used to estimate apparent elastic modulus, overall specimen stiffness, and apparent yield stress, with models typically having approximately 25–30 million elements. We found that ultrasound parameters were correlated with mechanical properties with R=0.70–0.82 ($p < 0.001$). Multiple regression analysis indicated that ultrasound measurements provide additional information regarding mechanical properties beyond that provided by bone quantity alone ($p \leq 0.05$). Adding ultrasound variables to linear regression models based on bone quantity improved adjusted squared correlation coefficients from 0.65 to 0.77 (stiffness), 0.76 to 0.81 (apparent modulus), and 0.67 to 0.73 (yield stress). These results indicate that ultrasound can provide complementary (to bone quantity) information regarding mechanical behavior of cancellous bone.

### Keywords

ultrasound; mechanical; cancellous; calcaneus; bone strength; finite element analysis; micro-CT

## 1. Introduction

Quantitative ultrasound (QUS) is a low-cost, portable, non-ionizing alternative to dual energy x-ray absorptiometry (DXA) [1–4]. An official position paper by the International

Corresponding author: Keith A. Wear, Food and Drug Administration, Center for Devices and Radiological Health, Bldg. 62, Room 2104, 10903 New Hampshire blvd., Silver Spring, MD 20993, (301) 796-2538, keith.wear@fda.hhs.gov.

Society for Clinical Densitometry (ISCD) states that QUS at the calcaneus can “predict fragility fracture in postmenopausal women (hip, vertebral and global fracture risk) and men over the age of 65 (hip and all non-vertebral fractures), independently of central DXA bone mineral density (BMD)” [5] A recommendation statement from the U.S. Preventive Services Task Force states that QUS at the calcaneus “predicts fractures of the femoral neck, hip, and spine as effectively as DXA” [6].

Despite the comparable effectiveness of the two modalities, the ISCD position paper also states that “Discordant results between heel QUS and central DXA are not infrequent and are not necessarily an indication of methodological error” [5]. (In this reference, “central DXA” refers to measurements at the spine and femur). One source of discordance is that QUS and DXA are performed at different skeletal sites. Another source of discordance is differences in the physics of ultrasound and x-rays. Although both modalities are highly sensitive to the quantity of bone intercepted by the beam, they may exhibit some disparity because of differences in the mechanisms underlying their interactions with bone.

In order to enhance diagnostic interpretation of calcaneal QUS measurements, there is motivation for investigating fundamental determinants of QUS measurements besides the most obvious one—bone quantity. At the richly trabecular calcaneus region, the mechanical properties associated with the ultrasound measurement depend primarily on bone quantity, trabecular microarchitecture, and trabecular-tissue material properties.

Most current clinical calcaneal bone sonometers measure two parameters in through-transmission through the heel: broadband ultrasonic attenuation (BUA) and speed of sound (SOS). Many studies have confirmed that these two parameters are good indicators of both bone mineral density (BMD) and fracture risk [5, 6]. One investigation found high correlations (R = 0.84 – 0.88) between normalized BUA (nBUA) and mechanical properties of human calcaneus [7]. To the best of the authors’ knowledge, no other studies have been performed to relate QUS parameters to mechanical properties of human calcaneus. Such studies are important in order to corroborate the earlier finding by Langton *et al.* and also to assess the correlations of mechanical properties with other QUS parameters, including SOS, broadband ultrasound backscatter (BUB), and dispersion (*i.e.*, the rate of change of phase velocity with frequency). BUB is not currently used clinically, but many studies suggest its feasibility and utility [8–11]. In addition, investigation into the relationships between QUS parameters and mechanical properties can provide insight into mechanisms underlying the interaction between ultrasound and cancellous bone, which could help inform future system design as bone sonometry technology evolves.

The first goal of this work was to measure how well ultrasound measurements predict mechanical properties of human calcaneus samples. The second goal was to evaluate how well ultrasound measurements in combination with bone quantity predict mechanical properties of human calcaneus samples, compared with predictability performance based on bone quantity alone.

## 2. Materials and methods

Ultrasound and mechanical properties were measured on 25 defatted human calcaneus samples (age and gender unknown) so that relationships between the two types of physical properties could be elucidated. Ultrasound properties were measured in water tank experiments involving through-transmission and pulse-echo methods. Mechanical properties were estimated using finite element analysis (FEA). Micro computed tomography (micro-CT) was performed to generate three-dimensional reconstructions of trabecular bone structure to be used as inputs to FEA. Micro-CT also provided estimates of bone volume fraction (BV/TV), which is a measure of bone quantity, to be used in multiple regression analysis to investigate whether ultrasound measurements provide additional information for the prediction of mechanical properties beyond that provided by bone quantity alone.

### 2.1 Bone samples

The sample preparation procedure has been described previously [12]. Defatting, which has been reported to have a small effect on ultrasound measurements [7, 13–16], was accomplished with a trichloro-ethylene solution. The lateral cortical layers were removed, leaving two parallel surfaces with direct access to trabecular bone. Calcaneal cortical layers are thin (a few mm thick) and have been reported to have a small effect (15%) on measurements of broadband ultrasound attenuation [17]. A thin layer of cortical bone remained along the other surfaces of the bone. This cortical layer (see periphery of bone sample in Figure 1) was excluded from regions of interest for the ultrasound measurements and all micro-CT analyses. The mean sample thickness was 1.8 cm (standard deviation = 0.2 cm).

### 2.2 Ultrasound Measurements

The ultrasound measurement methods have been reported previously [12]. Bone samples were interrogated in a water tank by ultrasound propagating in the mediolateral (or lateromedial) direction, as is the case with commercial bone sonometers. A Panametrics (Waltham, MA) 5800 pulser/receiver and Panametrics V301 broadband circular transducers (diameter = 2.54 cm, focal length = 3.81 cm, and center frequency = 500 kHz) were used. Received signals were digitized (8 bit, 10 MHz) using a LeCroy (Chestnut Ridge, NY) 9310C Dual 400 MHz oscilloscope and stored on computer (via GPIB) for off-line analysis.

Normalized broadband ultrasonic attenuation (nBUA), speed of sound (SOS), and dispersion were measured using a through-transmission method [12]. Normalized BUA was computed as the slope of a least-squares linear regression of attenuation coefficient (dB/cm) vs. frequency [7] from 300 to 700 kHz. This frequency range is typical for clinical bone sonometers. As is common in clinical and investigational bone sonometry, the parameter chosen for SOS was signal velocity rather than phase or group velocity. Relationships among various velocity measures have been described previously [12, 18]. Signal velocity was measured using the third zero crossing in advance of the pulse envelope maximum to mark time-of-arrival, which was near the leading edge of the pulse.

Four to eight ultrasound measurements were performed on each calcaneus sample by sequentially repositioning the ultrasound transducer between consecutive measurements, as shown in Figure 1. Results from all 4–8 measurements on a sample were averaged in order to fully represent a volume that would approximate the rectangular-shaped analysis volume used for micro-CT analysis.

Dispersion was measured by taking the slope of a linear regression to phase velocity vs. frequency from 300 to 700 kHz. Although dispersion is generally positive in soft tissues [19], it is usually negative in cancellous bone [20–24]. Negative dispersion may be due to multiple scattering [25–27] or interference between fast and slow waves that propagate in porous media [28–36].

Backscatter coefficients were measured using a reference phantom method [37, 38]. Backscatter coefficient vs. frequency data were least-squares fit to a power law over the range from 300 kHz to 700 kHz. The midband (500 kHz) value of the power law fit was used to describe broadband ultrasound backscatter (BUB). One important feature of the backscatter coefficient is that it is a fundamental material property of the scattering target (in this case, bone) and is independent of the measurement system, which is why it is a preferred index of scattering in biomedical applications [39]. Other indexes of scattering, such as apparent integrated backscatter (AIB), are useful but depend not only on the scattering properties of the target but also transducer geometry, diffraction effects, and attenuation effects.

Feasibility and utility of backscatter has been demonstrated in clinical trials at the calcaneus, in which the backscatter parameters were relative (*i.e.*, not compensated for attenuation) backscatter coefficient [8], BUB [9], average backscatter coefficient [40], and AIB [10]. Clinical measures of backscatter are usually not compensated for unknown transmission losses at the soft tissue / bone interface [8–10, 40]. Backscatter is sensitive to trabecular thickness [41–46], collagen and mineral content [47], mechanical properties [48, 49], bone mineral density [46, 50], and apparent density [51–54] in human cancellous bone. It is possible to compensate backscatter measurements for the presence of the cortical shell [55].

### 2.3 Micro-CT

Micro Computed Tomography (Scanco μCT 100, Scanco Medical, Basserdorf, Switzerland) was used to obtain three-dimensional (3D) trabecular microstructure of the calcaneus specimens. Figure 2 shows a reconstructed micro-CT image of a rectangular volume from a calcaneus sample. After the ultrasound measurements had been performed, cancellous bone samples were cut to approximately 2.0 cm × 4.0 cm × 1.8 cm and imaged at an isotropic voxel size of 17.2 μm (nominal resolution). (Specimens were not cut along the thickness dimension, which was maintained at approximately 1.8 cm.) An interior volume, approximately 1.8 cm × 3.6 cm × 1.6 cm was used for micro-structural analysis. A constant threshold to distinguish trabecular bone from background was chosen through histogram analysis of each specimen. The threshold was designated at a value below the broad peak in the histogram corresponding to trabeculae [56]. Trabecular microstructure such as bone volume fraction (BV/TV), trabecular thickness (Tb.Th), trabecular spacing (Tb.Sp),

trabecular number (Tb.N), connectivity density (Conn.D.), structure model index (SMI), and degree of anisotropy (DA) were quantified using previously published methods [57–58].

### 2.4 Finite element analysis

Finite element analysis (FEA) based on micro computed tomography (micro-CT) reconstructions is now established as an effective way to assess mechanical properties of trabecular bone samples [59–60]. FEA can be linear or nonlinear. Linear FEA can provide estimates of stiffness and apparent elastic modulus, while nonlinear FEA can also provide estimates of yield stress. Elastic modulus has been reported to be well correlated with strength over a range of bone densities [61–63]. However, yield stress may be a superior indicator of strength since failure behavior generally involves nonlinear phenomena such as local material yielding and geometrically large deformations [59].

The FEA simulations [64] employed a finite plasticity material model for trabecular bone [65, 66]. This involved a rate independent elasto-plasticity model [67, 68], previously proposed for modeling solids with elastic-plastic type stress-strain behavior at the macroscopic scale, but applied here at the level of individual trabeculae. The model included linear, isotropic hardening. A rate-type constitutive law was used to define kinematic hardening. Tension-compression asymmetry in trabecular tissue yield strength was incorporated using pseudo-kinematic hardening.

Using previously described methods, [59], the FEA simulations used eight-noded brick “voxel” (cube-shaped) elements and were performed at a down-sampled resolution of 34 μm. (A comparison on a subset of 11 calcaneus samples for 34 vs. 17 μm resolution confirmed a high level of agreement (always within 3%) between the two estimates of mechanical parameters, justifying use of the lower resolution.) In brief, all bone elements were assigned the same homogeneous and isotropic tissue material properties: elastic modulus 18GPa and Poisson’s ratio of 0.3 tensile yield strain of 0.33% and compressive yield strain of 0.81% [59, 64]. Both material and geometric (large deformation) non-linearities were allowed. Displacement-type boundary conditions were used to apply 1% apparent-level compressive strain. Models contained 7 to 44 million elements and were solved using a highly scalable, implicit parallel finite-element framework-Olympus [69] running on a Dell Linux Cluster supercomputer (Stampede, Texas Advanced Computing Center).

The FEA-loading direction was the long axis of the samples. However, it is understood that loading patterns for calcaneus *in vivo* are complex and not as unidirectional as, say, vertebrae. Outcomes included overall stiffness, defined as the ratio of the reaction force to the applied displacement from the linear response; apparent modulus, as the corresponding modulus for the whole specimen; apparent yield stress, defined using the 0.2% offset method; and the corresponding apparent yield strain.

### 2.5 Statistical Analysis

A variety of statistical tests were used. We performed univariate least squares regressions with BV/TV and each of the four ultrasound properties (nBUA, SOS, BUB, and dispersion)

as independent variables and each of the three mechanical properties (stiffness, apparent modulus, and yield stress) as dependent variables (for a total of 3 × 5 = 15 regressions).

We also compared how well bone quantity in combination with ultrasound measurements predicted mechanical properties. For those comparisons, multiple regressions were performed in which the dependent variable was a mechanical property and the independent variables were BV/TV and each one of the $2^4 = 16$ possible combinations of the four ultrasound measurements (nBUA, SOS, BUB, dispersion). This process was performed for each of the three mechanical properties as dependent variables (for a total of 3 × 16 = 48 regressions).

The additive value of each ultrasound parameter (nBUA, SOS, BUB, dispersion) for assessing mechanical properties of calcaneus samples (beyond that provided by BV/TV) was assessed by the p-value for that parameter in the mulitple regression (which included BV/TV as another independent variable). Goodness of fit of multiple regressions was measured by the adjusted coefficient of determination, $R_a$, which is related to the correlation coefficient, $R$, by $R_a^2 = 1 - (1 - R^2)(n - 1) / (n - m - 1)$ where $n$ = total number of data points and $m$ = number of independent variables in regression model [70]. This approach is similar to that taken by Chaffai *et al.* in multiple regression models to predict ultrasound parameters (nBUA, SOS, and BUB) from BMD and histomorphometric parameters [41]. Another statistical parameter that has been used to assess goodness of fit for multiple regressions is the Mallows $C_p$ statistic [70, 71], which is closely related to $R_a$ [72]. In all analyses, $p<0.05$ was taken as the level of statistical significance, and no account was made in the assumed level of statistical significance for performing multiple comparisons. Ninety-five percent confidence intervals for correlation coefficients were computed by assuming that the transformed variable $z = \log_e[(1+R) / (1-R)]/2$ was approximately normally distributed [73].

## 3. Results

Table 1 shows means and standard deviations of morphometric properties of the 25 calcaneus samples. These values are similar to those reported by Ulrich *et al.* for human calcaneus [74].

Figure 3 shows FEA predictions of failed bone tissue in compression (blue) and tension (red) for the cancellous bone samples, with bone volume fractions (BV/TV) shown below each sample. The images show the considerable heterogeneity of human calcaneus and a variety of failure locations. Figure 4 shows scatter plots and least-squares regression linear fits for ultrasound measurements versus mechanical properties in human cancellous bone samples. Table 2 shows correlation coefficients ($R$) and 95% confidence intervals. The ultrasound parameters—particularly nBUA, SOS, and BUB—are moderately correlated with mechanical properties of cancellous bone. nBUA, SOS, and BUB were all positively correlated with mechanical properties and BV/TV. However, dispersion was negatively correlated with mechanical properties and BV/TV.

Table 3 shows results for multivariate regression models to predict mechanical properties from linear combinations of bone quantity (BV/TV) and ultrasound measurements. As

expected, most (65 – 76%) of the variations in mechanical properties could be explained by variations in bone quantity (BV/TV) ($p < 0.0001$). The p values for added ultrasound variables suggest that BUB and SOS provided more additional information to BV/TV than nBUA and dispersion. The fact that nBUA provided less additional information to BV/TV than either BUB or SOS could partially result from nBUA exhibiting a higher correlation (than either BUB or SOS) to BV/TV (which is supported by Table 2) and therefore was more redundant in a statistical sense. Adjusted $R^2$ values suggest that the additional variance in mechanical properties explained by the combination of bone volume fraction plus ultrasound parameters beyond that explained by only bone volume fraction was $\Delta R_{adj}^2$ = 12% (stiffness), 5% (apparent modulus), and 6% (yield stress).

## 4. Discussion

Quantitative ultrasound can be approximately as effective as DXA-measured BMD for assessing risk of fracture [6, 75]. Specifically, in a landmark prospective hip-fracture study involving 5662 elderly women [75], BUA and SOS in calcaneus predicted the risk of hip fracture as well as did DXA, and after controlling for the femoral neck BMD, the ultrasonographic variables remained predictive of hip fracture. Other clinical studies have reported similar findings [76, 77]. Moayyeri *et al.* reported a meta-analysis involving 21 studies and follow-up of 279,124 person-years that indicated that heel ultrasound adjusted for hip BMD showed a significant and independent association with fracture risk [78]. Our finding that nBUA and SOS correlated well ($0.64 < R^2 < 0.72$) with bone quantity (BV/TV) partly explains ultrasound's success in assessing fracture risk since bone strength and fracture risk are clearly related to bone mass and BMD. In addition, our finding that combining ultrasound parameters with bone quantity had greater associations with mechanical properties than did univariate models based on bone quantity alone suggests that these ultrasound measurements can indeed detect some aspect of mechanically-relevant bone quality, presumably some aspect of the microarchitecture since the finite element models did not reflect any variations in material quality. Similarly, Hans *et al.* [70] and Moayyeri *et al.*, [77] reported that adding heel ultrasound measurements to hip BMD improved hip [70] and total [77] fracture risk assessment in a clinical trials. However, unlike these studies, our study featured site-matched measurements. Also consistent with our findings, Chaffai *et al.* showed that ultrasound measurements at calcaneus carry some information regarding microarchitecture beyond that contained in BMD [41]. Taken together, these findings provide insight into why ultrasonographic variables have been associated with risk of hip fracture independent of hip BMD. The present study helps to elucidate mechanisms underlying clinical findings.

Comparing our results with the literature, Table 4 shows correlation coefficients between ultrasound and mechanical properties for three studies in human cancellous bone at frequencies near 500 kHz. The correlation coefficients in the present study for nBUA were much closer to values reported by Langton *et al.* in calcaneus (n=20) [17] than those reported by Hakulinen *et al.* in medial condyle of femur (n=10) and medial plateau of tibia (n=10) [49]. However, at four higher frequencies, ranging from 1 – 5 MHz, Hakulinen *et al.* found higher correlations between nBUA and Young's modulus (0.29 – 0.56) and ultimate strength (0.31 – 0.71) but still not as high as the correlations between nBUA and mechanical

properties reported by Langton *et al.* or in the present investigation. The correlations reported in the present study for SOS and BUB near 500 kHz with mechanical properties in calcaneus tended to be higher than those reported by Hakulinen *et al.* in tibia and femur. However, as with nBUA, the correlations reported by Hakulinen *et al.* at the four higher frequency ranges tended to be higher for SOS (0.58 – 0.82) and BUB (0.55 – 0.74) and were sometimes comparable to correlations reported in the present study. Karjalainen *et al.*, found similar correlations between BUB and ultimate strength in the higher frequency ranges (0.46 – 0.76) for human proximal tibia (n = 10) and distal femur (n = 10) [48]. (Karjalainen *et al.* did not report measurements near 500 kHz and did not report measurements of nBUA, SOS, or dispersion.)

Differences in experimental methods may partially explain disparities in correlation coefficients between ultrasound and mechanical properties. The present study and the study by Langton *et al.* measured calcaneus in the mediolateral orientation, with ultrasound propagation perpendicular to the predominant trabecular orientation. In contrast, the studies by Hakulinen *et al.* and Karjalanen *et al.* measured tibia and femur, and the angle between the ultrasound propagation and the predominant trabecular orientation was unclear. Another potential source of disparity among the studies is the degree of co-registration of tissue volumes for ultrasound and mechanical measurements, which remains a challenging aspect for these kinds of investigations (as discussed below). Correlations would be expected to decline as co-registration of ultrasound and mechanical measurement volumes diminishes.

The micro-CT-based FEA methodology used in this study has been well validated for predicting strength of trabecular bone cores taken from multiple anatomic sites [79] but nonetheless has some limitations [59]. First, since the models assumed homogeneity of the bone tissue within and across specimens they did not consider variance in apparent-level mechanical properties due to any variance in tissue-level material properties, either within or among bone samples [79]. Therefore, the present results do not reflect any such real variations. Second, our specimens were quite heterogeneous microstructurally, which tended to focus failure locally in those regions of lowest bone volume fraction. Such effects likely diminish the role of BV/TV of the entire specimen on its overall mechanical behavior, but this may actually be representative of real *in vivo* behavior as such regions of low bone volume fraction do exist in highly osteoporotic individuals. And as noted above, we did not assess femoral or vertebral bone in this study. However, ultrasound is used only at the calcaneus and thus our measurements reflect assessment of the bone that is most relevant for this technology.

One limitation of this study specific to the use of ultrasound is that the ultrasound beam did not interrogate bone samples uniformly throughout the volume of interest. The ultrasound beam intensity at the focal plane for a focused circular transducer is not uniform but rather is distributed according to an Airy pattern, which is maximum near the axis of the transmitter and decreases with distance from the axis. A further complication is that the beam width was frequency dependent. At the low end of the transducer band, 300 kHz, the diameter of the central lobe, $2.44\lambda z/d$ [80], was 18 mm, which was commensurate with the width of the micro-CT reconstruction volume. At the high end of the transducer band, 700 kHz, the diameter of the central lobe was 8 mm. Therefore, the ultrasound measurements were always

weighted toward the center region of the sample, with this effect becoming more pronounced as frequency increased from 300 to 700 kHz. The effect of this spatial weighting of ultrasound measurements could have been to decrease correlations with mechanical properties that had different spatial weighting throughout the volume of interest. In addition, since backscatter data were gated to exclude specular reflections at the front surfaces of calcaneus samples, backscatter volumes of interest were a few millimeters smaller in the thickness dimension than nBUA, SOS, BV/TV, and FEA volumes of interest.

This study involved purely cancellous samples and therefore did not consider the role of cortical bone. It is common practice to remove or avoid cortical layers in bone samples in order to elucidate properties of cancellous bone, including ultrasonic [3, 7, 11–17, 22–24, 27–29, 38, 42] and mechanical [59, 60, 62–64, 79] properties.

The sample size for this study (n = 25) was sufficient to establish that ultrasound parameters provide important additive information to bone quantity. Further study involving larger sample sizes is warranted in order to better quantify the magnitude of this additive information.

## 5. Conclusion

Correlations between ultrasound parameters and mechanical properties of human cancellous calcaneus were investigated, with nBUA, SOS, and BUB showing high correlations and dispersion showing a moderate correlation. Ultrasound parameters provided information beyond that provided by bone quantity alone for the prediction of mechanical properties of cancellous bone.

## Acknowledgements

This work was supported by the FDA Office of Women's Health. Computational resources were made available through the National Science Foundation's XSEDE program (Grant TG-MCA00N019. The authors also gratefully acknowledge the technical assistance of Shashank Nawathe, Ph.D. The mention of commercial products, their sources, or their use in connection with material reported herein is not to be construed as either an actual or implied endorsement of such products by the Department of Health and Human Services.

## References

[1]. Langton CM, Palmer SB, and Porter RW. The measurement of broadband ultrasonic attenuation in cancellous bone. Eng Med 13 (1984) 89–91. [PubMed: 6540216]

[2]. Laugier P Instrumentation for in vivo ultrasonic characterization of bone strength. IEEE Trans Ultrason. Ferroelectr. Freq. Contr 55 (2008) 1179–1196.

[3]. Laugier P Quantitative ultrasound instrumentation for bone in vivo characterization In: Laugier P, Haiat G, editors. Bone quantitative ultrasound, New York: Springer; 2011, p. 47–72.

[4]. Barkmann R and Glüer CC. Clinical applications In: Laugier P, Haiat G, editors. Bone quantitative ultrasound, New York: Springer; 2011, p. 73–82.

[5]. Krieg MA, Barkmann R, Gonnelli S, Stewart A, Bauer DC, Barquero LDR, et al. Quantitative ultrasound in the management of osteoporosis: The 2007 ISCD Official Positions. J. Clin. Densitom 11 (2008) 163–187. [PubMed: 18442758]

[6]. U. S. Preventive Services Task Force. Screening for Osteoporosis: U.S. Preventive Services Task Force recommendation Statement. Ann. Intern. Med 154 (2011) 356–365. [PubMed: 21242341]

[7]. Langton CM, Njeh CF, Hodgskinson R, Currey JD. Prediction of mechanical properties of the human calcaneus by broadband ultrasonic attenuation. Bone 18 (1996) 495–503. [PubMed: 8805988]

[8]. Wear KA and Garra BS. Assessment of bone density using ultrasonic backscatter. Ultrasound Med. & Biol, 24 (1998) 689–695. [PubMed: 9695272]

[9]. Roux C, Roberjot V, Porcher R, Kolta S, Dougados M, Laugier P Ultrasonic backscatter and transmission parameters at the os calcis in postmenopausal osteoporosis. J Bone Miner Res 16 (2001) 1353–1362. [PubMed: 11450712]

[10]. Jiang Y, Liu C, Li R, Wang W, Ding H, Qing Q et al., Analysis of apparent integrated backscatter coefficient and backscattered spectral centroid shift in calcaneus in vivo for the ultrasonic evaluation of osteoporosis. Ultrasound Med. & Biol, 40 (2014) 1307–1317. [PubMed: 24642217]

[11]. Wear KA. Ultrasonic scattering from cancellous bone: a review. IEEE Trans. Ultrason. Ferro. Freq. Cont 55 (2008) 1432–1441.

[12]. Wear KA. The effects of frequency-dependent attenuation and dispersion on sound speed measurements: applications in human trabecular bone. IEEE Trans. Ultrason. Ferro. Freq. Contr 47 (2000) 265–273.

[13]. Alves JM, Ryaby JT, Kaufman JJ, Magee FP and Siffert RS. Influence of marrow on ultrasonic velocity and attenuation in bovine trabecular bone. Calcif Tissue Int. 58 (1996) 362–367. [PubMed: 8661972]

[14]. Njeh CF and Langton CM. The effect of cortical endplates on ultrasound velocity through the calcaneus: an in vitro study. Br J Radiol 70 (1997) 504–510. [PubMed: 9227233]

[15]. Nicholson PHF and Bouxsein ML. Bone marrow influences quantitative ultrasound measurements in human cancellous bone. Ultrasound Med & Biol 28 (2002) 369–375. [PubMed: 11978417]

[16]. Hoffmeister BK, Auwarter JA and Rho JY. Effect of marrow on the high frequency ultrasonic properties of cancellous bone. Phys Med Biol 47 (2002) 3419–3427. [PubMed: 12375829]

[17]. Xia Y, Lin W, and Qin YX. The influence of cortical end-plate on broadband ultrasound attenuation measurements at the human calcaneus using scanning confocal ultrasound. J. Acoust Soc Am 118 (2005) 1801–1807.

[18]. Haiat G, Padilla F, Cleveland RO, and Laugier P Effects of frequency-dependent attenuation and velocity dispersion on in vitro ultrasound velocity measurement in intact human femur specimens. IEEE Trans Ultrason. Ferror. Freq. Contr 53 (2006) 39–51.

[19]. O'Donnell M, Jaynes ET, and Miller JG. Kramers-Kronig relationship between ultrasonic attenuation and phase velocity. J. Acoust. Soc. Am, 69 (1981) 696–701.

[20]. Nicholson PH, Lowet G, Langton CM, Dequeker J, Van der Perre G. Comparison of time-domain and frequency-domain approaches to ultrasounic velocity measurements in trabecular bone. Phys. Med. Biol 41 (1996) 2421–2435. [PubMed: 8938036]

[21]. Strelitzki R and Evans JA. On the measurement of the velocity of ultrasoiund in the os calcis using short pulses. Eur J. Ultrasound 4 (1996) 205–213.

[22]. Droin P, Berger G, and Laugier P Velocity dispersion of acoustic waves in cancellous bone. IEEE Trans Ultrason Ferroelectr Freq Contr 45 (1998) 581–592.

[23]. Wear KA. Measurements of phase velocity and group velocity in human calcaneus. Ultrasound in Med. & Biol, 26 (2000) 641–646 [PubMed: 10856627]

[24]. Lee KI. Correlations of group velocity, phase velocity, and dispersion with bone density in bovine trabecular bone. J. Acoust. Soc. Am 130 (2011) EL399–EL404 [PubMed: 22225133]

[25]. Wear KA. The dependences of phase velocity and dispersion on trabecular thickness and spacing in trabecular bone-mimicking phantoms. J. Acoust. Soc. Am, 118 (2005) 1186–1192. [PubMed: 16158673]

[26]. Haiat G, Lhemery A, Renaud F, Padilla F, Laugier P, and Naili S. Velocity dispersion in trabecular bone: influence of multiple scattering and of absorption. J. Acoust. Soc. Am 124 (2008) 4047–4058. [PubMed: 19206827]

[27]. Wear KA. The dependencies of phase velocity and dispersion on volume fraction in cancellous-bone-mimicking phantoms. J. Acoust. Soc. Am 125 (2009) 1197–1201. [PubMed: 19206892]

[28]. Hosokawa A and Otani T. Ultrasonic wave propagation in bovine cancellous bone. J. Acoust. Soc. Am, 101 (1997) 558–562. [PubMed: 9000743]

[29]. Hosokawa A and Otani T. Acoustic anisotropy in bovine cancellous bone. J. Acoust. Soc. Am, 103 (1998) 2718–2722. [PubMed: 9604363]

[30]. Kaczmarek M, Kubik J, and Pakula M. Short ultrasonic waves in cancellous bone. Ultrasonics 40 (2002) 95–100. [PubMed: 12160076]

[31]. Fellah ZEA, Chapelon JY, Berger S, Lauriks W, and Depollier C. Ultrasonics wave propagation in human cancellous bone: application of Biot theory. J. Acoust. Soc. Am, 116 (2004) 61–73. [PubMed: 15295965]

[32]. Nagatani Y, Mizuno K, Saeki T, Matsukawa M, Sakaguchi T, and Hosoi H. Numerical and experimental study on the wave attenuation in bone – FDTD simulation of ultrasound propagation in cancellous bone. Ultrasonics 48 (2008) 607–612. [PubMed: 18589470]

[33]. Anderson CC, Marutyan KR, Holland MR, Wear KA, and Miller JG. Interference between wave modes may contribute to the apparent negative dispersion observed in cancellous bone. J. Acoust. Soc. Am, 124 (2008) 1781–1789. [PubMed: 19045668]

[34]. Pakula M, Padilla F, Laugier P, and Kaczmarek M. Application of Biot's theory to ultrasonic characterization of human cancellous bones: Determination of structural, material, and mechanical properties. J. Acoust. Soc. Am 123 (2008) 2415–2423. [PubMed: 18397044]

[35]. Fujita F, Mizuno K, and Matsukawa M. An experimental study on the ultrasonics wave propagation in cancellous bone: Waveform changes during propagation. J. Acoust. Soc. Am 134 (2013) 4775–4781. [PubMed: 25669289]

[36]. Hosokawa A. Numerical Investigation of reflection properties of fast and slow longitudinal waves in cancellous bone. IEEE Trans. Ultrason. Ferro. Freq. Contr 60 (2013) 1030–1035.

[37]. Yao LX, Zagzebski JA, and Madsen EL. Backscatter coefficient measurements using a reference phantom to extract depth-dependent instrumentation factors. Ultrason. Imaging 12 (1990) 58–90. [PubMed: 2184569]

[38]. Wear KA. Frequency dependence of ultrasonic backscatter from human trabecular bone: theory and experiment, J. Acoust. Soc. Am 106 (1999) 3659–3664. [PubMed: 10615704]

[39]. Wear KA, Stiles TA, Frank GR, Madsen EL, Cheng F, Feleppa EJ, Hall CS, Kim BS, Lee P, O'Brien WD, Oelze ML, Raju BI, Shung KK, Wilson TA, and Yuan JR. Interlaboratory comparison of ultrasonic backscatter coefficient measurements from 2 to 9 MHz. J. Ultrasound Med 24 (2005) 1235–1250. [PubMed: 16123184]

[40]. Wear KA and Armstrong DW. Relationships among calcaneal backscatter, attenuation, sound speed, hip bone mineral density, and age in normal adult women. J. Acoust. Soc. Am, 110 (2001) 573–578. [PubMed: 11508981]

[41]. Chaffai S, Peyrin F, Nuzzo S, Porcher R, Berger G, and Laugier P. Ultrasonic characterization of human cancellous bone using transmission and backscatter measurements: relationships to density and microstructure. Bone 30 (2002) 229–237. [PubMed: 11792590]

[42]. Wear KA and Laib A. The relationship between ultrasonic scattering and microarchitecture in human calcaneus. IEEE Trans Ultason Ferro Freq Cont. 50 (2003) 979–986.

[43]. Padilla F, Peyrin F and Laugier P Prediction of backscatter coefficient in trabecular bones using a numerical model of three-dimensional microstructure. J. Acoust. Soc. Am, 113 (2003) 1122–1129. [PubMed: 12597205]

[44]. Padilla F, Jenson F, and Laugier P Estimation of trabecular thickness using ultrasonic backscatter. Ultrason Imag 26 (2006) 3–22.

[45]. Hakulinen MA, Day JS, Toyras J, Weinans H, and Jurvelin JS. Ultrasonic characterization of human trabecular bone microstructure. Phys Med Biol 51 (2006) 1633–1648 [PubMed: 16510968]

[46]. Malo MKH, Toyras J, Karjalainen JP, Isaksson H, Riekkinen O, Jurvelin JS. Ultraosnic backscatter measurements of intact human proximal femurs—relationships of ultrasound parameters with tissue structure and mineral density. Bone 64 (2014) 240–245. [PubMed: 24769331]

[47]. Hoffmeister BK, Whitten SA, Kaste SC, and Rho JY. Effect of collagen and mineral content on the high-frequency ultrasonic properties of human cancellous bone. Bone 13 (2002) 26–32.

[48]. Karjalainen JP, Toyras J, Riekkinen O, Hakulinen M, Jurvelin JS. Ultrasound backscatter imaging provides frequency-dependent information on structure, composition and mechanical properties of human trabecular bone. Ultrasound Med. & Biol, 35 (2009) 1376–1384. [PubMed: 19525060]

[49]. Hakulinen MA, Day JS, Toyras J, Timonen M, Kroger H, Weinans H et al. Prediction of density and mechanical properties of human trabecular bone *in vitro* by using ultrasound transmission and backscattering measurements at 0.2 – 6.7 MHz frequency range. Phys. Med. & Biol 50 (2005) 1629–1642. [PubMed: 15815086]

[50]. Ta D, Wang W, Huang K, Wang Y, and Le LH. Analysis of frequency dependence of ultrasonic backscatter coefficient in cancellous bone. J. Acoust. Soc. Am, 124 (2008) 4083–4090. [PubMed: 19206830]

[51]. Hoffmeister BK, Whitten SA, and Rho JY. Low-megahertz ultrasonic properties of bovine cancellous bone. Bone. 26 (2000) 635–642. [PubMed: 10831936]

[52]. Hoffmeister BK. Frequency dependence of apparent ultrasonic backscatter from human cancellous bone. Phys Med Biol 56 (2011)67–683.

[53]. Lee KI KI and Choi MJ. Frequency-dependent attenuation and backscatter coefficients in bovine trabecular bone from 0.2 to 1.2 MHz. J. Acoust. Soc. Am 131 (2012)EL67–EL73. [PubMed: 22280732]

[54]. Hoffmeister BK, Wilson AR, Gilbert MJ, and Sellers ME. A backscatter difference technique for ultrasonic bone assessment. J. Acoust. Soc. Am, 132 (2012) 4069–4067. [PubMed: 23231136]

[55]. Liu C, Ta D, Hu B, Le L, Wang W. The analysis and compensation of cortical thickness effect on ultrasonic backscatter signals in cancellous bone. J. Appl. Phys, 116 (2014) 124903.

[56]. Follet H, Bruyere-Garnier K, Peyrin F, Roux JP, Arlot ME, Burt-Pichat B, Rumelhart C, and Meunier PJ, Relationship between compressive properties of human os calcis cancellous bone and microarchitecture assessed from 2D and 3D synchrotron microtomography, Bone, 36 (2005) 340–351. [PubMed: 15780961]

[57]. Hildebrand T and Ruegsegger P. A new method for the model-independent assessment of thickness in three-dimensional images. Journal of Microscopy-Oxford (1997) 185:67–75

[58]. Hildebrand T, Laib A, Muller R, Dequeker J, and Ruegsegger P Direct three-dimensional morphometric analysis of human cancellous bone: microstructural data from spine, femur, iliac crest, and calcaneus. J Bone Miner Res 14 (1999) 1167–1174 [PubMed: 10404017]

[59]. Bevill T and Keaveny TM. Trabecular bone strength predictions using finite element analysis of micro-scale images at limited spatial resolution. Bone 44 (2009) 579–584. [PubMed: 19135184]

[60]. Wang J, Zhou B, Liu XS, Fields AJ, Sanyal A, Shi X, et al. Trabecular plates and rods determine elastic modulus and yield strength of human trabecular bone. Bone 72 (2015) 71–80. [PubMed: 25460571]

[61]. Keaveny TM, Wachtel EF, Ford CM, Hayes WC. Differences between the tensile and compressive strengths of bovine tibial trabecular bone depend on modulus. J Biomech 27 (1994) 1137–46. [PubMed: 7929463]

[62]. Fyhrie DP and Schaffler MB. Failure mechanisms in human vertebral cancellous bone. Bone 15 (1994) 105–109. [PubMed: 8024844]

[63]. Morgan EF and Keaveny TM. Dependence of yield strain of human trabecular bone on anatomic site. J Biomech 34 (2001) 569–77. [PubMed: 11311697]

[64]. Bevill G, Eswaran SK, Gupta A, Papapodoulos P, and Keaveny TM: Influence of bone volume fraction and architecture on computed large-deformation failure mechanisms in human trabecular bone. Bone 39 (2006) 1218–1225. [PubMed: 16904959]

[65]. Papadopoulos P and Lu J. A general framework for the numerical solution of problems in finite elasto-plasticity. Comput Methods Appl Mech Eng 159 (1998) (1–2):1–18.

[66]. Papadopoulos P and Lu J. On the formulation and numerical solution of problems in anisotropic finite plasticity. Comput Methods Appl Mech Eng 190 (2001) 4889–910.

[67]. Green AE and Naghidi PM. A general theory of an elastic-plastic continuum. Arch Rat Mech Anal 18 (1965) 251–81.

[68]. Green AE and Naghidi PM. Some remarks on elastic-plastic deformation at finite strain. Int J Eng Sci 9 (12) (1971) 1219.

[69]. Adams MF, Bayraktar HH, Keaveny TM and Papadopoulos P. Ultrascalable implicit finite element analyses in solid mechanics with over a half a billion degrees of freedom ACM/IEEE Proceedings of SC2004: high performance networking and computing. Washington, DC: IEEE Computer Society; 2004.

[70]. Zar JH, Biostatistical Analysis, Prentice-Hall, Upper Saddle River, NJ, 2010, chapter 20, section 428.

[71]. Draper NR and Smith H. Applied Regression Analysis, John Wiley & Sons, Inc., New York, New York, 1998, chapter 15.

[72]. Kennard RW. A note on the $C_p$ statistic. Technometrics, 13,(1971) 899–900.

[73]. Hoel PG. Introduction to Mathematical Statistics, John Wiley & Sons, Inc., New York, New York, 1962, chapter 7.

[74]. Ulrich D, van Rietbergen B, Laib A, and Ruegsegger P. The ability of three-dimensional structural indices to reflect mechanical aspects of trabecular bone, Bone 25, (1999) 55–60. [PubMed: 10423022]

[75]. Hans D, Dargent-Molina P, Schott AM, Sebert JL, Cormier C, Kotzki PO, Delmas PD, Pouilles JM, Breart G, and Meunier PJ. Ultrasonic heel measurements to predict hip fracture in elderly women: the EPIDOS prospective study, Lancet 348 (1996) 511–514. [PubMed: 8757153]

[76]. Hans D, Schott AM, Duboeuf F, Durosier C, and Meunier PJ, Does follow-up duration influence the ultrasound and DXA predication of hip fracture? The EPIDOS prospective study, Bone, 35, (2004) 357–363. [PubMed: 15268884]

[77]. Moayyeri A, Kaptoge S, Dalzell N, Luben RN, Wareham NJ, Bingham S, Reeve J, and Khaw KT. The effect of including quantitative heel ultrasound in models for estimation of 10-year absolute risk of fracture, Bone 45 (2009) 180–184. [PubMed: 19427923]

[78]. Moayyeri A, Adams JE, Adler RA, Krieg MA, Hans D, Compston J, and Lewiecki EM. Quantitative ultrasound of the heel and fracture risk assessment: an updated meta-analysis, Osteo. Int 23 (2012)143–153.

[79]. Bevill G, Eswaran SK, Farahmand F and Keaveny TM: The influence of boundary conditions and loading mode on high-resolution finite element-computed trabecular tissue properties. Bone, 44 (2009) 573–8. [PubMed: 19110082]

[80]. Goodman JW. Introduction to Fourier Optics. San Francisco: McGraw-Hill 1968.

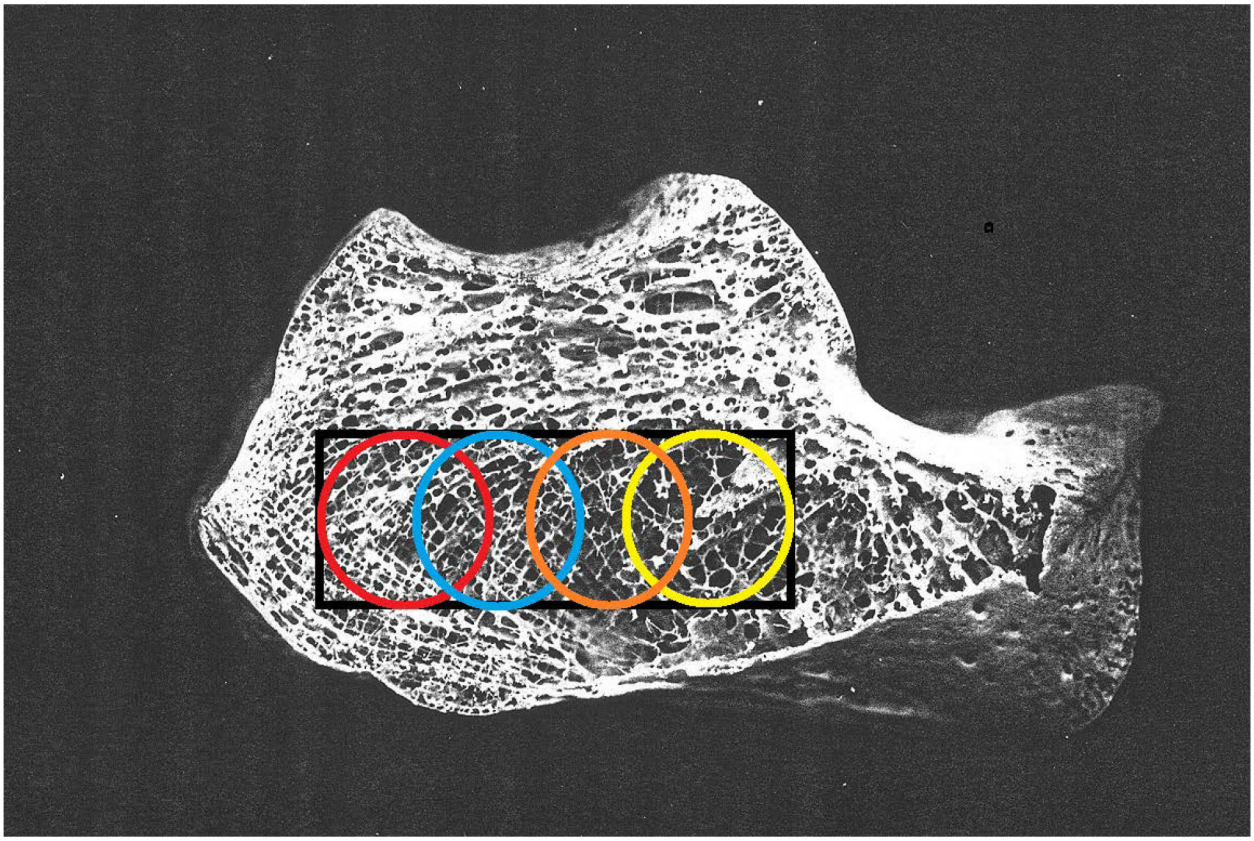

**Figure 1.**
Calcaneus sample. The circles represent ultrasound beam cross-sections for repeated measurements as the ultrasound transducer was sequentially repositioned. The ultrasound measurements from a series of 4–8 locations were averaged in order to approximate the rectangular volume used for micro-CT. After ultrasound measurements, the rectangular volume was cut out for micro-CT analysis.

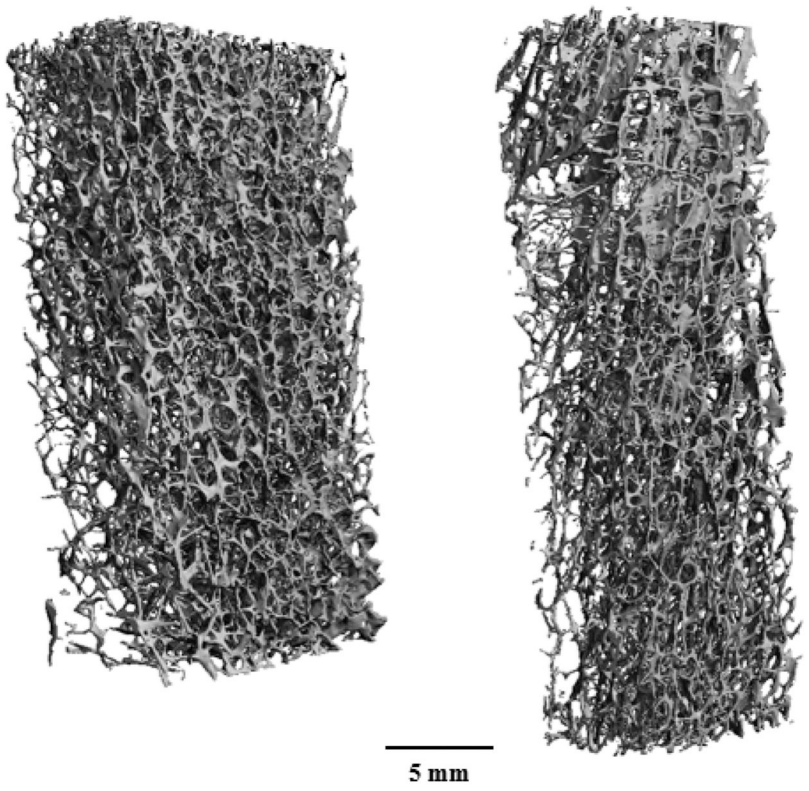


**Figure 2.**
Micro-CT reconstructions from calcaneus specimens. The BV/TV values are 0.074 (left) and 0.060 (right).

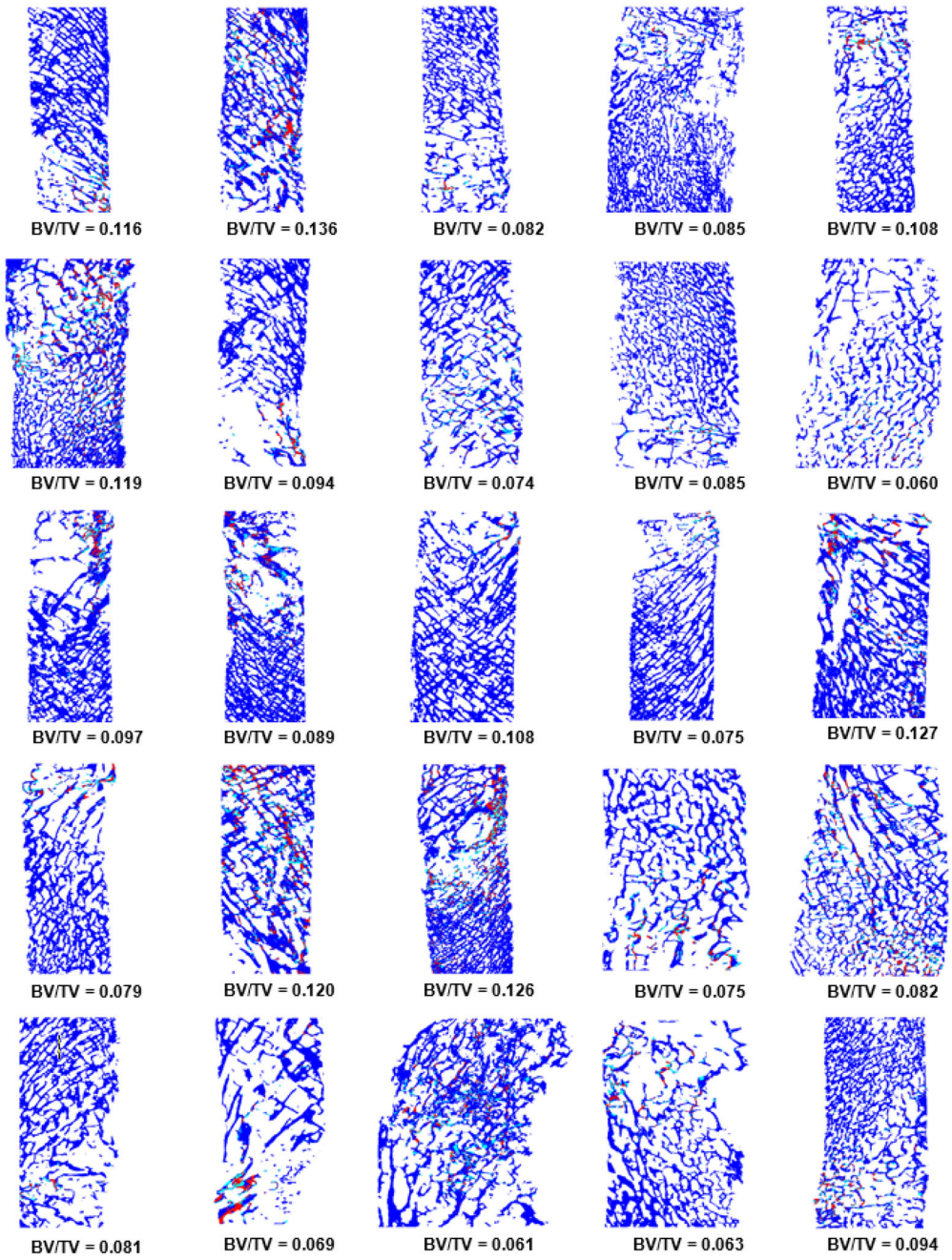


**Figure 3.**

FEA of bone samples. The images show predictions of failed tissue in compression (light blue) and tension (red) for all 25 cancellous bone samples. The bone volume fraction BV/TV is shown below each sample.

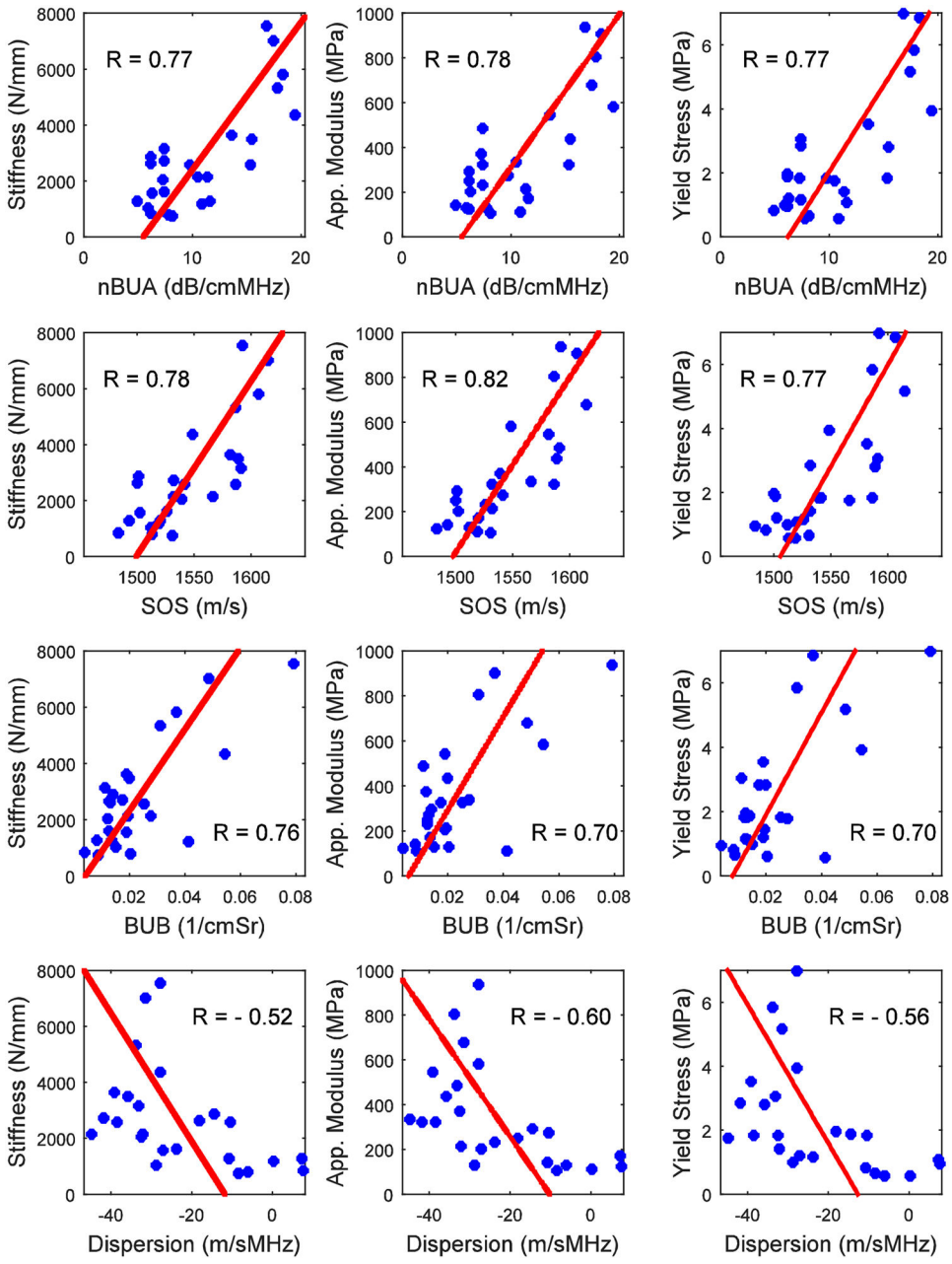


**Figure 4.**

Scatter plots of the measured ultrasound parameters vs. the FEA-derived mechanical properties in 25 human cancellous calcaneus samples.

**Table 1.**

Morphometric properties of 25 human calcaneus specimens.

| Parameter | Symbol | Mean ± Standard Deviation |
|---|---|---|
| Bone Volume Fraction | BV/TV | 0.092 ± 0.022 |
| Bone Surface Fraction (1/mm) | BS/BV | 21.7 ± 2.7 |
| Trabecular Thickness (μm) | Tb.Th | 127 ± 16 |
| Trabecular Number (1/mm) | Tb.N | 0.98 ± 0.15 |
| Trabecular Spacing (mm) | Tb.Sp | 1.01 ± 0.17 |
| Structural Model Index | SMI | 1.60 ± 0.32 |
| Connectivity Density | Conn.D | 3.74 ± 1.24 |
| Degree of Anisotropy | DA | 1.64 ± 0.11 |

**Table 2.**

Correlation coefficients between ultrasonic and mechanical properties of human cancellous bone.

| Ultrasound Parameter | Correlation Coefficient (R) | | | |
|---|---|---|---|---|
| | BV/TV | Stiffness | Apparent Modulus | Yield Stress |
| nBUA | 0.85[a] (0.68–0.93) | 0.77[a] (0.54–0.90) | 0.78[a] (0.55–0.90) | 0.77[a] (0.52–0.89) |
| SOS | 0.80[a] (0.59–0.91) | 0.78[a] (0.55–0.90) | 0.82[a] (0.62–0.92) | 0.77[a] (0.54–0.90) |
| BUB | 0.64[b] (0.32–0.83) | 0.76[a] (0.52–0.89) | 0.70[b] (0.41–0.86) | 0.70[a] (0.42–0.86) |
| Dispersion | −0.53[c] (−0.77–−0.16) | −0.52[c] (−0.77–−0.15) | −0.60[c] (−0.81–−0.26) | −0.56[c] (−0.77–−0.15) |

Values in parentheses indicate 95% confidence intervals.

*a*: $p \leq 0.0001$.

*b*: $p \leq 0.001$.

*c*: $p \leq 0.01$.

**Table 3.**

Values of adjusted $R^2$ for multivariate regression models to predict mechanical properties from linear combinations of bone quantity (BV/TV) and ultrasound measurements.

| Input Multiple Regression Variable(s) | Output Regression Variable | | | | | |
|---|---|---|---|---|---|---|
| | Stiffness | | Apparent Modulus | | Yield Stress | |
| | $R_{adj}^2$ | p value for ultrasound variable | $R_{adj}^2$ | p value for ultrasound variable | $R_{adj}^2$ | p value for ultrasound variable |
| BV/TV | 0.65[a] | | 0.76[a] | | 0.67[a] | |
| BV/TV, nBUA | 0.66[a] | 0.23 | 0.75[a] | 0.53 | 0.67[a] | 0.34 |
| BV/TV, SOS | 0.68[a] | 0.07[e] | 0.79[a] | 0.05[d] | 0.70[a] | 0.12 |
| BV/TV, BUB | 0.76[a] | 0.01[c] | 0.78[a] | 0.08[e] | 0.71[a] | 0.05[d] |
| BV/TV, dispersion | 0.65[a] | 0.37 | 0.78[a] | 0.11 | 0.68[a] | 0.22 |
| BV/TV, SOS, BUB | 0.77[a] | | 0.81[a] | | 0.73[a] | |

The p values for the added ultrasound variables in multiple regressions are shown.

*a:* $p \leq 0.0001$.

*b:* $p \leq 0.001$.

*c:* $p \leq 0.01$.

*d:* $p \leq 0.05$.

*e:* $p \leq 0.10$.

**Table 4.**

Correlation coefficients between ultrasound and mechanical properties for three studies in human cancellous bone.

| | Elasticity | | | | Strength | | |
|---|---|---|---|---|---|---|---|
| **Study** | **[7]** | **[49]** | **This paper** | | **[7]** | **[49]** | **This paper** |
| **Site** | **Calcaneus** | **Femur & Tibia** | **Calcaneus** | | **Calcaneus** | **Femur & Tibia** | **Calcaneus** |
| n | 20 | 20 | 25 | | 20 | 20 | 25 |
| Frequency Range (kHz) | 200–600 | 300–600 | 300–700 | | 200–600 | 300–600 | 300–700 |
| Mechanical Parameter | Young's Modulus | Young's Modulus | Apparent Modulus | Stiffness | Strength | Ultimate Strength | Yield Stress |
| nBUA (95% CI) | 0.88 | 0.05 | 0.78 (0.55–0.90) | 0.77 (0.54–0.90) | 0.84 | 0.03 | 0.77 (0.52–0.89) |
| SOS (95% CI) | | 0.57 | 0.82 (0.62–0.92) | 0.78 (0.55–0.90) | | 0.60 | 0.77 (0.54–0.90) |
| BUB (95% CI) | | 0.54 | 0.70 (0.41–0.86) | 0.76 (0.52–0.89) | | 0.71 | 0.70 (0.54–0.90 |
| Dispersion (95% CI) | | | −0.60 (−0.81–−0.26) | −0.52 (−0.77–−0.15) | | | −0.56 (−0.77–−0.15) |

The table shows results obtained in a range of frequencies relevant for clinical bone sonometers. Note that, at four higher frequency ranges, within 1 – 5 MHz, Hakulinen *et al.* found higher correlations between nBUA and Young's modulus (0.29 – 0.56) and ultimate strength (0.31 – 0.71).